Research Square

Preprints are preliminary reports that have not undergone peer review.
They should not be considered conclusive, used to inform clinical practice,
or referenced by the media as validated information.

Surrogate modeling based on CFD data as a way to handle the large parameter space of propeller-wing interactions

Michael Schollenberger

michael.schollenberger@iag.uni-stuttgart.de

University of Stuttgart https://orcid.org/0009-0007-7225-2142

Maximilian Kern

University of Stuttgart

Mário Firnhaber Beckers

University of Stuttgart

Thorsten Lutz

University of Stuttgart

Research Article

Keywords: Aerodynamic Interactions, Distributed Propulsion, Numerical Simulation, Surrogate Modeling

Posted Date: November 18th, 2026

DOI: https://doi.org/10.21203/rs.3.rs-11768710/v1

License: This work is licensed under a Creative Commons Attribution 4.0 International License.
Read Full License

Additional Declarations: The authors declare no competing interests.

Surrogate modeling based on CFD data as a way to handle the large parameter space of propeller-wing interactions

M. Schollenberger[1], M. Kern[1], M. Firnhaber Beckers[1], L. Lutz[1]

Abstract
The paper examines the use of simple surrogate models extrapolated from CFD data at a few sampling points to incorporate the aerodynamic interactions of distributed propulsion in aircraft design. The surrogate models are generated with the open source *Surrogate Modeling Toolbox* (SMT). The studies are based on high-fidelity numerical simulations with the second order finite volume flow solver TAU, developed by the German Aerospace Center (DLR), employing Reynolds-Averaged Navier-Stokes (RANS) equations. To reduce the computational effort, a 2.5D approach was used in which a single propeller was simulated in front of a wing segment and the propeller was modeled by an actuator disk (ACD). Examined is the influence of three parameter for positioning the distributed propellers on the aerodynamic efficiency and the excess power efficiency. A sampling methods (Design of Experiment (DoE)) is used to determine where CFD simulations should be performed to obtaining a deep insight into the full parameter space with as little numerical effort as possible. The surrogate models generated from the CFD database are evaluated in terms of their accuracy. To this end, comparisons are made with CFD simulations that were not used to generate the surrogate model. Thus, the use of surrogate models to capture the large parameter space of distributed propulsion concepts is discussed and evaluated.

Keywords Aerodynamic Interactions, Distributed Propulsion, Numerical Simulation, Surrogate Modeling

List of Symbols

x, z	streamwise, vertical coordinate	m
Θ	inclination angle	deg
Ω	rotational speed angle	s^{-1}
Re	Reynolds number	-
M	Mach number	-
V	velocity	m/s
c	chord length	m
η	propulsive efficiency	-
D	drag	N
L	lift	N
P	power	W
T	thrust	N
W	weight	N
F	force	N
Q	torque	Nm
$C_{...}$	global coefficient	-

Indices

∞	inflow
prop	propeller
ex	excess

Indices

∞	inflow
eff	effective
S	Shaft

Abbreviations

AoA	Angle of Attack
ACD	Actuator Disk
BC	Boundary Condition
BET	Blade Element Theory
BL	Boundary Layer
DoE	Design of Experiment
DP	Distributed Propulsion
FF	Full Factorial
WTP	Wingtip mounted Propeller
CFD	Computational Fluid Dynamics
RANS	Reynolds Averaged Navier-Stokes equations
RPM	Rotation per minute
SA	Spalart–Allmaras turbulence
SM	Surrogate Model
SMT	Surrogate Modeling Toolbox

1 Introduction

A key approach to developing more sustainable aircraft is to increase the overall efficiency by utiliz-

Michael Schollenberger
schollenberger@iag.uni-stuttgart.de

[1] University of Stuttgart, Institute of Aerodynamics and Gas Dynamics, Wankelstraße 3, D-70563 Stuttgart, Germany

ing positive aerodynamic interactions between the propulsion system and the aircraft. Distributed propulsion (DP) and wingtip mounted propellers (WTP) are recent examples of this approach [4, 9]. However, studies on such novel concepts are characterized by a large, multidimensional parameter space and require high-fidelity numerical methods (CFD) to capture the various interactions with sufficient accuracy. This leads to difficulties in aircraft design. The simplified methods of classic aircraft design, based on analytical estimations, low-fidelity numerical methods or and empirical correlations, can no longer be used. Analytical estimations of interaction effects do not exist, simplified numerical methods are often times qualitatively insufficient in their representation of the flow physics, while CFD methods are too computationally intensive for design iterations. Furthermore, known empirical correlations cannot be used because they are derived from conventional configurations.

Another characteristic of propeller-wing interactions is that the breakdown of traditional disciplines in aviation is coming to an end. Aerodynamics and propulsion technology are no longer separable, as the airflow around the wings directly affects the thrust T and shaft power P_S of the propellers, and the propeller slipstream can change both the lift L and drag D forces on the wings. The wing can be characterized by the aerodynamic efficiency $\eta_{aero} = L/D$ and the propeller by the propulsive efficiency $\eta_{prop} = T\ V_\infty/P_s$ as the ratio of the thrust times the flight velocity V_∞ to the shaft power. Taking aerodynamic interactions into account is therefore crucial when designing novel aircraft, since they affect both efficiencies. For cruise flight optimization the product of both efficiencies, known as the aero-propulsive efficiency $\eta_{ap} = \eta_{aero} \cdot \eta_{prop}$, is thus the relevant parameter for aircraft design since it incorporates all relevant efficiencies and forces taking the aerodynamic interactions into account [1].

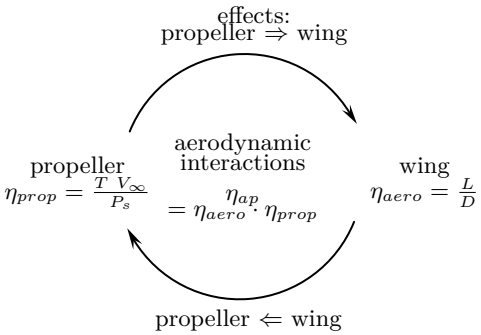


Fig. 1: Principle of the aerodynamic interaction between a propeller and a wing

CFD can capture the interaction effects an the aero-propulsive efficiency quite well. However, directly incorporating high-fidelity numerical simulations into aircraft design is far too time-consuming. In general, aerodynamic data sets generated from CFD can usually be incorporated into aircraft design either in the form of look-up tables or by using simple surrogate models (SM), which rudimentary represent the influence of various parameters on the aerodynamic coefficients by extrapolating the CFD data from a few sampling points. The use of SM in aircraft design as such is therefore not a new approach. However, when using SMs in aircraft design in combination with novel configurations, it is important to validate the reliability of the SMs in capturing the impact of the aerodynamic interactions. Using a CFD-fitted SM for aircraft design must represent the aero-propulsive efficiency to a reliable degree. As part of the LuFo project VELAN, extensive parameter studies have already been carried out on the influence of the propeller position in a DP configuration. Based on existing parameter studies on the positioning of DP propellers in front of the wing for a generic regional aircraft, various SMs are evaluated in this paper with regard to their ability to capture the effect of the aerodynamic interactions on the aero-propulsive efficiency for DP in cruise flight.

2 Methodology and Numerical Setup

When designing new aircraft configurations with DP, the relative positioning between the propellers and the wing is important. As various studies have shown [3, 7], the effects of the propeller on the wing, as well as the effects of the wing on the propeller, are very sensitive to the propeller position. The streamwise position $(x/c)_{prop}$, the vertical position $(z/c)_{prop}$ and the angle of inclination θ between the propellers and the wing, see Figure 2, were found to be significant factors. These parameters span a three-dimensional parameter space $((x/c)_{prop}, (z/c)_{prop}, \theta)$, which is to be reproduced by SM.

To generate and validate SM based on CFD data, simulations of a generic regional aircraft (comparable to ATR 42 or C-295) equipped with DP are performed. The assumed inflow conditions for the generic DP configuration are a Mach number of $M = 0.44$ ($V_\infty = 139\ m/s$) and a Reynolds number of $Re = 11.45 \cdot 10^6$ based on the chord length of $c = 1.98$ at a temperature of 249.0 K (altitude approx. 6 km). A NACA-65(3)-218 airfoil is used, see Beckers [3]. The propeller has a diameter of $D = 2\ m$ at a rotational speed of approximately 2,000 RPM. To reduce the computational effort, a 2.5D approach

is used in which a single propeller was simulated in front of a wing segment of 2.5 m spanwise length. The 2.5D model follows the setup of Beckers [3]. The model allows the local positions to be studied exemplarily for the entire aircraft, since the propeller position as well as the inclination angle can be alternated.

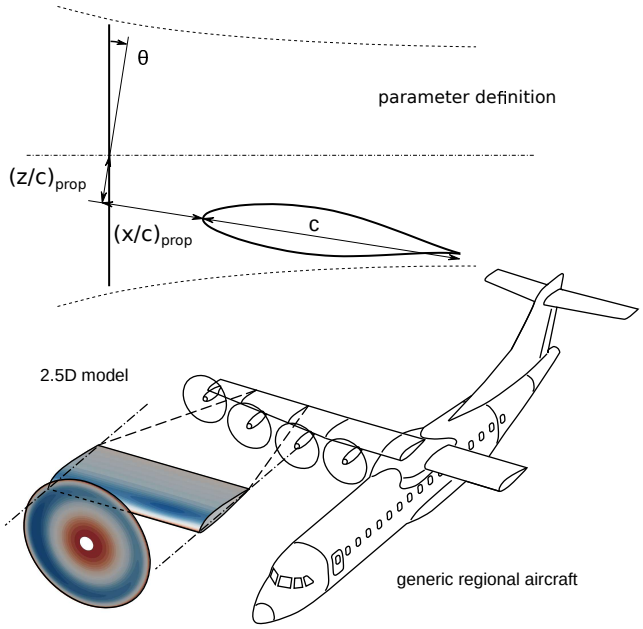


Fig. 2: Parameter definition and 2.5D model approach

2.1 Numerical Setup

The numerical simulations in this study were performed using the second-order finite volume flow solver TAU developed by the German Aerospace Center (DLR) [8], which solves Reynolds-Averaged Navier-Stokes (RANS) equations. The influence of the propellers on the wing is modeled by a steady-state Actuator Disc (ACD) method [5] based on a boundary condition (BC). The turbulence was modeled with the Spalart Allmaras turbulence model. All simulations are performed fully turbulent neglecting a possible effect of the propeller slipstream on the laminar turbulent transition and a possible increase in viscous drag due to reduced laminar lengths. Due to the low Mach number, preconditioning was used in the TAU simulations. A trimming algorithm was used to ensure force equilibrium for steady-state cruise conditions (thrust equals drag and lift equals weight) in the simulation by iteratively adjusting the propeller rotational speed and the global angle of attack (AoA), see Figure 6. The algorithm was used before [7].
The program XROTOR was used to design the generic propeller. XROTOR, developed by Drela and Youngren [2], is a propeller design and analysis program which generates propeller geometries for minimum induced loss conditions. It is based on the classical blade-element/vortex formulation.

2.1.1 Actuator Disk

The TAU ACD generates non-uniform axial and tangential velocity profiles to achieve a physically correct representation of the propeller slipstream influence on the wing. A blade element theory (BET) based force calculation within the ACD model takes into account the influences of the wing on the propeller as well. Thus, the 2.5D method is able to capture both the influence of the propeller slipstream on the wing and vice versa of the wing on the propeller forces. The axial and tangential forces are equivalent to those of the propeller (averaged over one propeller revolution) and are introduced via a circular infinitesimally thin disc. The stationary approach of the ACD enables an enormous reduction in computational time compared to fully-resolved propeller simulations. Propeller polars are used as input data for the ACD, generated via the propeller design tool XROTOR by varing the inflow conditions and a subsequent post-processing.

2.1.2 Numerical Grid

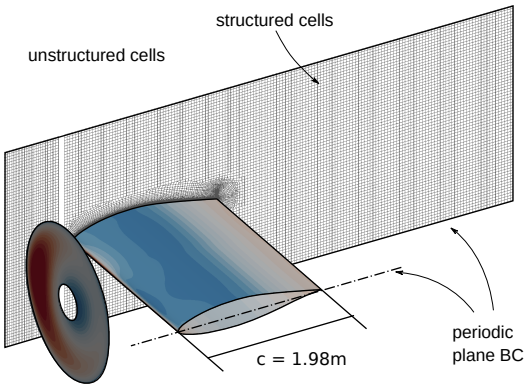


Fig. 3: Numerical grid of the eGenius-Mod half wing

Hybrid grids are used for the 2.5D model, shown in Figure 3, with structured cells in the BL of the wing, the area of the propeller slipstream, and the wing wake. Unstructured cells are utilized in the farfield. The inflow and outflow is realized by a farfield BC at a distance of $100c$. Periodic boundary conditions (BC) are applied at the side boundaries. In this way an infinite wing with an infinite number of co-rotating propellers can be modeled. For the propeller grid a cylindrical approach is used. The quasi Cartesian wake area has a mesh resolution corresponding to a cell size of $\approx 2\%$ relative to the wing chord c to preserve the slipstream until it passes over the wing.

The grid for the 2.5D model has a total number of points of ≈ 4 million, depending on the specific propeller positions and the inclination angle.

2.1.3 Cruise Algorithm

A trimming algorithm is used to adjust cruise conditions in the CFD simulation, see Figure 6. It combines two iteration loops to reach lift and weight ($L = W$) equilibrium by an AoA iteration and thrust and drag ($T = D$) equilibrium by a rotational speed (RPM) iteration. For the AoA iteration, a TAU-internal loop is used which adjusts to a specified effective lift coefficient $C_{L,eff}$. For the rotational speed iteration, TAU is embedded in an additional external loop where a secant method is used to adjust the thrust to the aircraft drag determined by CFD. To achieve cruise flight conditions in the 2.5D model, the thrust-drag difference is iterated towards a prespecified excess thrust F_{ex}, corresponding approximately to the drag components of the overall aircraft (mainly fuselage and empenage drag as well as the wing's induced drag), which are not captured in the 2.5D approach. Thus, it is basically a zero point search for the function $T - D = F_{ex}$. The trimmed 2.5D model thus corresponds to cruise conditions. The influence of the interactions on the aircraft drag is therefore taken into account in the thrust and drag equilibrium.
The calculation procedure is: first, a fully converged TAU calculation is performed with the RPM of the isolated propeller design data. Then, a second TAU calculation is started with a 10% reduced RPM. This allows the secant method to start the thrust iteration loops. In each loop around 1000-1500 iterations are calculated at a constant rotational speed with the TAU-internal AoA iteration before the rotational speed is then varied.

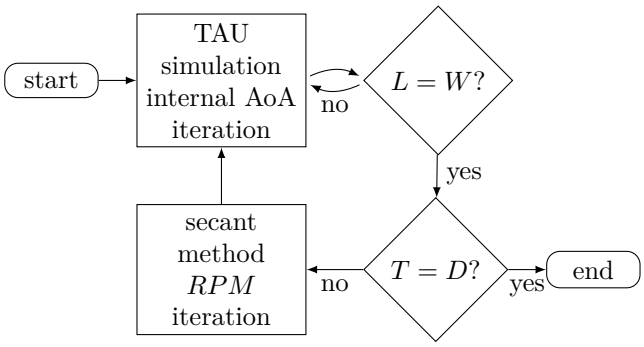


Fig. 4: Flowchart of the cruise algorithm

2.2 Methodology

To select the CFD data for the SM generation, a Design of Experiments (DoE) approach is used to identify combinations of parameters that are sufficient to cover the entire parameter space with a relatively small number of simulations. Based on these so called sampling points, SMs are then generated, which are used for comparison with manually conducted CFD sweeps (1D slices trough the parameter space along one parameter while the other two are fixed).

2.2.1 Design of Experience

DoE is a statistical sampling method for creating a reduced data set within a large parameter space. The investigated parameter space ($(x/c)_{prop}$, $(z/c)_{prop}$, θ), shown in Table 1, is resolved in five different levels within the limits shown in Figure 5.

parameter	min	max
$(x/c)_{prop}$ [-]	-1	-0.3
$(z/c)_{prop}$ [-]	-1	0.5
θ [°]	2	12

Tab. 1: Limits of the parameter space investigated

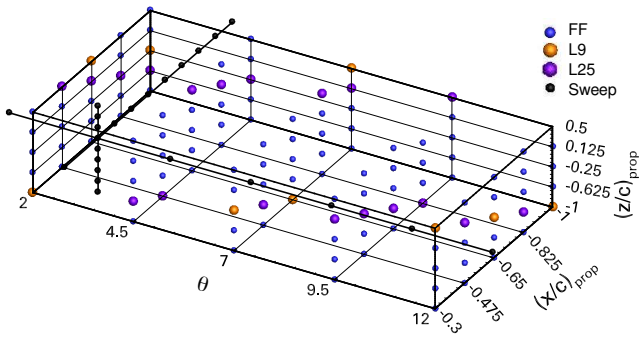


Fig. 5: Visualization of the 3D parameter space including the DoE sampling points and the manually generated sweeps

The number of possible combinations with three parameters (also called factors in DoE) and five levels is $5^3 = 125$. The use of all possible combinations is also referred to as full factorial (FF) analysis. In order to capture the characteristics of the design parameter while avoiding calculating all these possible combinations, the so-called Taguchi method is used for the DoE [10]. With this method, orthogonal arrays are formed within the design space (thus called partial factorial), which are assumed to allow the characteristics of the parameters to be determined. In these arrays, columns are orthogonal to each other, which means that all factor level combinations occur with equal frequency. In terms of probability theory, this ensures that all factors are taken into account in a balanced manner [10].
Standardized orthogonal arrays developed by Taguchi are used to create the DoE [10]. For three parameters and five levels, only 25 sampling points

are required using the so called L25 orthogonal array. In contrast to the FF design, the computational effort can thus be reduced to 20%. For comparison, a Taguchi L9 array with only three levels for the three parameters is considered as well, for which the computational effort with 9 simulations can be reduced even to 7.2% of the FF at 5 levels[1]. The DoEs considered thus always have three factors, but differing in the numbers of levels used.

2.2.2 Surrogate Model Building

Based on the sampling points of the DoE with the orthogonal arrays L9 and L25 as well as on the entire FF design, CFD simulations were performed using the 2.5D model. The CFD results of the DoE were then used as training points for the SM generation. The SM generation was performed with the *Python*-based open source *Surrogate Modeling Toolbox* (SMT) [6], developed by NASA and ONERA. The SMT was used to create kriging SM with a squared exponential correlation function (Gaussian) and a constant polynomial as the regression function. As input parameters of the SM generation, the effective aerodynamic efficiency L/D_{eff} and the excess power efficiency η_{ex} from the CFD simulations are used. The use of these two evaluation parameters is motivated by considering the overall aircraft in cruise flight. With the cruise conditions $T = D$ and $L = W$, the power consumption of an aircraft in cruise flight is given by $P_s = \frac{WV_\infty}{L/D\ \eta_{prop}}$. In this sense, the product of effective aerodynamic efficiency $\eta_{aero} = L/D$ and the propulsive efficiency η_{prop} as the so called aero-propulsive efficiency η_{ap} is the relevant parameter for the aircraft design. In the end, it's not the detailed phenomena that matter for aircraft design, but only the influences of the interactions on the aircraft's power requirements.

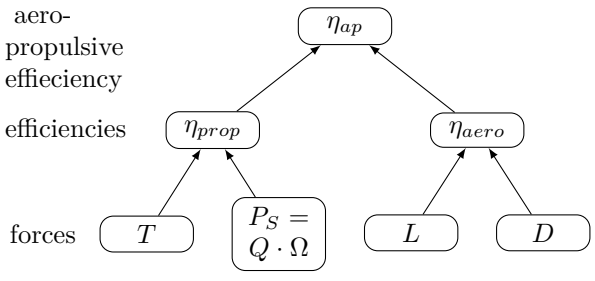


Fig. 6: Levels of evaluation parameter when considering aerodynamic interaction bewteen propeller and wings

A CFD-fitted SM for aircraft design thus has to represent this influence as the output values. For full aircraft simulation under strict cruise conditions, it would be sufficient to only use the aero-propulsive efficiency for the SM generation, as it would incorporate the efficiencies of the propellers and the wing as well as all relevant forces in one parameter.
However, since in this study a 2.5D model is used and cruise conditions are only approximated, the two effective efficiencies are used instead. The effective aerodynamic efficiency L/D_{eff} includes the vertical force components of the propeller in the effectively generated lift [3]. Depending on the interactions, the thrust vector of the propeller possesses a slight force in or against the direction of lift. By evaluating the effective aerodynamic efficiency L/D_{eff}, the change in lift and drag of the overall propeller-wing system can be thus be evaluated in combination. For the 2.5D model of one propeller in front of a wing segment the propeller generates a higher thrust than the wing segment drag, so no stationary flight condition is given. In terms of the power balance, this means that the thrust power is higher than the losses due to the wing. The difference is called excess power $P_{ex} = (T - D)V_\infty$. The excess power efficiency η_{ex} is build as the ratio of the excess power to the shaft power of the propeller, thus $\eta_{ex} = \frac{P_{ex}}{P_s}$. By evaluating the excess power efficiency η_{ex}, the changes in thrust and drag, can be considered in combination as well and corresponds to the propulsive efficiency of the whole aircraft in cruise flight.

3 Results and Discussion

The output of the SM on the basis of the DoE results (L9, L25, FF) for the three parameters are presented and discussed below. For the validation of the SM outside of the training points, manual parameter studies with only one variable parameter (sweeps) were also performed. By comparison with these, the SM are to be examined qualitatively and quantitatively depending on the number of training points used. The practicability is thus subsequently evaluated. The simulation results are obtained using the cruise algorithm and thus represent trimmed cruise conditions. The trimming algorithm sets all cases to a excess thrust of $1,350\ N$ and an effective lift coefficient $C_{L,eff} = 0.55$.

3.1 Surrogate Model Validation

The SMs output in general represent the entire 3D parameter space, so their response corresponds to a volume. To better visualize the results, however, Figure 7 shows an exemplary response surface through the parameter space at a constant $\theta = 3.2°$. The aerodynamic effective efficiency L/D is plotted over

[1] An FF with three levels would correspond to $3^3 = 27$ calculations, corresponding to 1/3 of the computational effort by using L9.

the two remaining free parameters $(x/c)_{prop}$ and $(z/c)_{prop}$. For comparison, the manually performed sweeps are shown (dashed black lines) and the slices through the response surface at the same locations are made visible (solid violet lines). It can be seen that the characteristics are basically captured by the SM. In order to better evaluate the SM qualitatively and quantitatively, however, the slices alongside all three parameters for the SMs are compared with the CFD sweeps in the following.

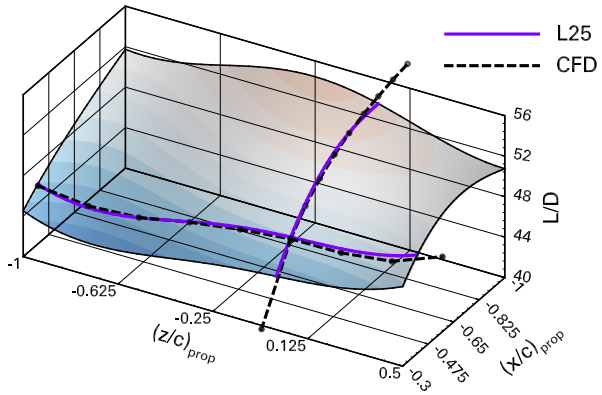


Fig. 7: Response surface $L/D((x/c)_{prop}, (z/c)_{prop})$ of the L25 SM with constant $\theta = 3.2°$ in comparison with the manual generated CFD sweeps alongside $(x/c)_{prop}$ and $(z/c)_{prop}$

Figure Figure 8 shows the results of the surrogate model formed from the DoE results for the three parameters $(x/c)_{prop}, (z/c)_{prop}, \theta$ along the three CFD parameter study sweeps. The aerodynamic efficiency is plotted on the left, and the excess efficiency on the right. The results of the CFD sweeps are shown as gray symbols, and the results of the SM as colored lines. The SM based on the L9 results is shown in orange, the one with the L25 results in purple, and the FF-based one in blue.

The CFD sweep results correspond to the results already found in previous studies on DP optimization [3, 7]. With regard to the streamwise propeller position, a larger distance from the wing leads to an increase in aerodynamic efficiency, but the excess efficiency and thus the power requirement remain constant beyond a certain distance ($(x/c)_{prop} \approx -0.5$). For the vertical positioning of the DP, it can be seen that over-the-wing arrangements lead to increased aerodynamic efficiency, but the highest efficiency and thus the lowest power requirement occur when positioned slightly below the wing ($(z/c)_{prop} \approx -0.2$), where the propeller benefits from the reduced inflow velocity due to the presence of the wing. For the inclination angle between the propeller and the wing, the optimum efficiency for the airfoil used is at $\theta \approx 6°$.

Two requirements must be satisfied in order to use SM for aircraft design: firstly, the qualitative progression of the sweeps must match that of the CFD sweeps; secondly, the optimums of the three design parameters must correspond with sufficient accuracy to the CFD values and be located at approximately the same position. The first requirement is important in order to be able to assess the influence of the aerodynamics in relation to other disciplines such as the structural mechanics or the flight mechanics in the overall design. The second is important for detecting the correct optimal positioning of the DP propellers. Comparing the aerodynamic efficiency and the excess power in Figure 8 with the CFD sweeps results shows that the qualitative progressions are reproduced well with the SM based on the L25 and FF DoE. The match of the FF SM is slightly in closer agreement, but the results of the L25 SM are almost as accurate, with a 80% reduction in computational effort. The largest difference between the FF and L25 results occurs in the excess efficiency of the vertical position. The SM based on the L9, on the other hand, cannot reproduce the results qualitatively. The qualitative progression of the aerodynamic efficiency over the three parameter shows a wrong mathematical behavior. For example, while L/D over the vertical position is W-shaped for the CFD data it is predicted to be linear with the L9 SM. On the other hand, where the CFD results show an almost linear behavior over the inclination angle, the L9 SM oscillates. An aircraft design based on the L9 results would be based on incorrect physical relationships.

With regard to the optimal position identified, the results in excess efficiency and the corresponding parameter location are shown in Table 2.

parameter	L9	L25	FF	CFD
$(x/c)_{prop}$ [-]	-	-1	-0.6	-0.6
$\Delta\eta_{ex}$ [%]	-0.16	-0.09	-0.06	-
$(z/c)_{prop}$ [-]	-0.25	-0.14	-0.17	-0.2
$\Delta\eta_{ex}$ [%]	0.21	-0.13	0.03	-
θ [°]	4	7	6.2	~ 6
$\Delta\eta_{ex}$ [%]	-0.19	-0.07	-0.02	-

Tab. 2: Position of the optimal DP propeller and SM value relative to CFD results

The accuracy increases with the number of CFD training points used for the SM generation. The efficiencies achieved for the SM with L25 and FF correspond very closely to those of the CFD optima. The L9 SM shows larger deviations, especially in the inclination angle, but still remains low. The FF SM is almost exact in determining the optimal positions. The L9, on the other hand, is unable to predict the decrease in efficiency for very close positions, as it assumes a constant progression. For example, the opti-

mum for the inclination angle would be determined at 4° instead of 6°, and the vertical positioning of the propeller would be too low.
In general, the validation with CFD sweeps shows that SM based on L25 and FF are capable of accurately reproducing the aerodynamic interactions in terms of both quality and quantity. The resolution of the DP parameter space with 5 levels is justified by the close agreement with the CFD sweeps. Due to the substantially reduced computational effort (only 20% compared to FF) and the nearly identical results ($\Delta \approx 0.1\%$), the L25 model is preferable for DP consideration in aircraft design. Even with the simple L9, the excess efficiency can be reproduced ($\Delta \approx 0.2\%$), but the prediction of the qualitative progression of the aerodynamic efficiency fails.

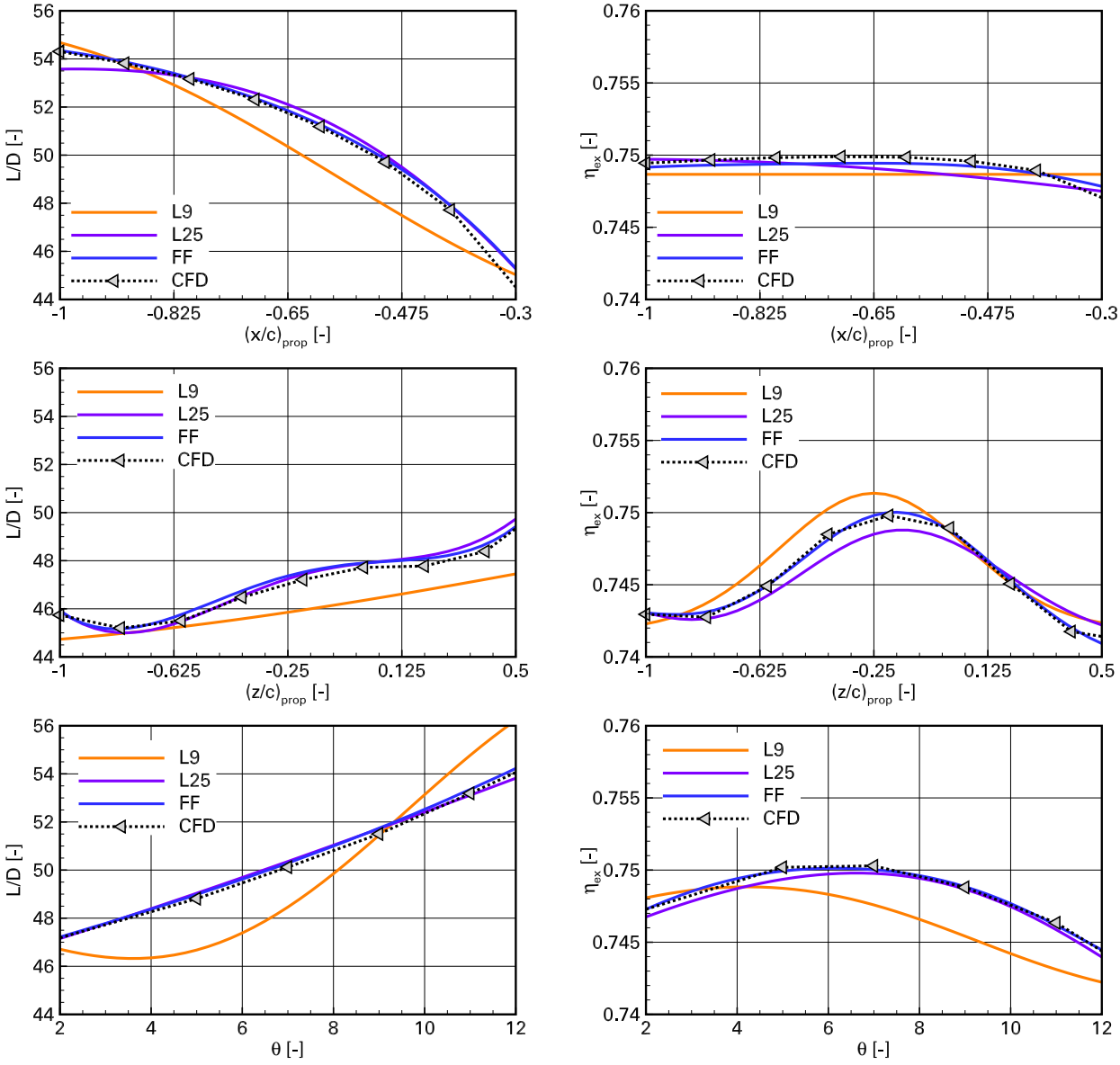


Fig. 8: Parameter study of the position and inclination angle of the WTP and the inner propeller

3.2 Sweep extended Surrogate Model Validation

In the investigation of novel configurations in collaboration between aerodynamics and aircraft design, it is common practice to first perform manual parameter studies in the form of CFD sweeps. This enables an understanding of the aerodynamic interactions without statistical uncertainty, as could result from purely relying on DoE. For this reason, the idea arises to use the existing CFD results of the manual sweeps and to only supplement these with DoE training points to generate SM. The additional

DoE points are therefore only needed to build a representation across the entire parameter space, which wouldn't be possible with sweeps alone.
To test this approach, new SMs were generated using the sampling points of the L9 and L25 DoE in combination with the manual sweep results, as well as one SM using only the sweeps as training points. The latter serves only visualization purposes, as unlike the DoE, the pure sweeps do not allow for a meaningful resolution of the parameter space. Duplicate positions, i.e., the intersection points of the sweeps, were removed for the SM training, which is a requirement for SM generation.

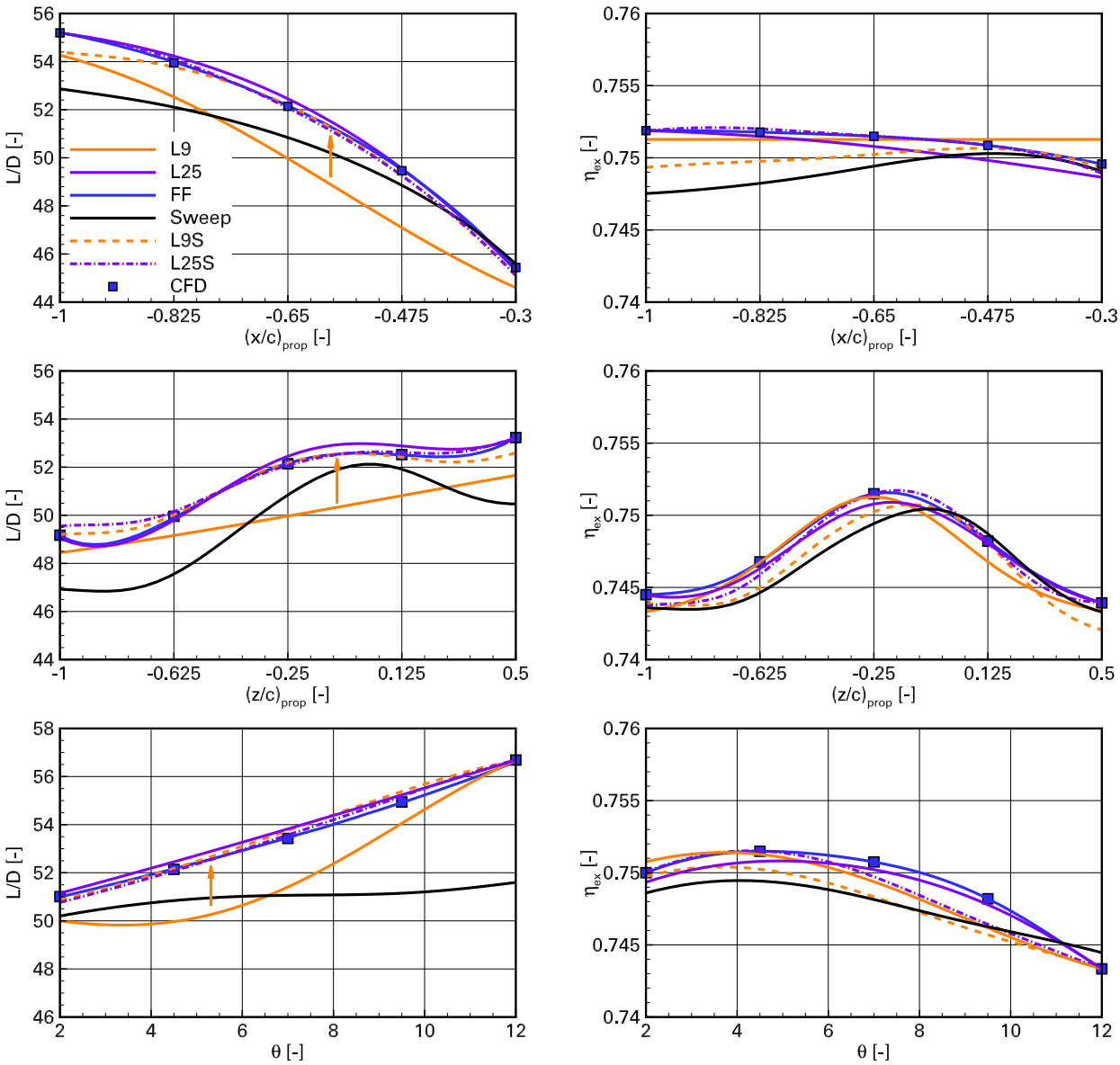


Fig. 9: Parameter study of the position and inclination angle of the WTP and the inner propeller

Figure 9 shows the results of the previous examined SM based only on the L9 and L25 results, as well as the versions extended by the sweeps (indicated with S). For comparison, the results of the FF SM and the underlying CFD results used to generate it, are also shown as validation data here. Three slices through the parameter space are shown again: for the evaluation of $(x/c)_{prop}$ at constant $(z/c)_{prop} = 0-0.25$ and for the $(z/c)_{prop}$ evaluation at constant $(x/c)_{prop} = -0.65$, each at constant $\theta = 4.5°$. The θ evaluation is performed accordingly at constant $(x/c)_{prop} = -0.65$ and $(z/c)_{prop} = 0 - 0.25$. The slices generated in this way correspond approximately to the positions of the optima identified above, i.e. to the FF sam-

pling points that are close to them. The same color scheme as above is used for the visualization: blue for the FF, violet for L25, and orange for L9. The SM based purely on the sweeps is shown in black. The SM based purely on the DoE data are shown as solid lines, those extended by the sweeps as dashed lines.
The evaluation of the aerodynamic efficiency L/D shows that the L9 and L25 models benefit from the inclusion of the CFD sweeps as training points. The L9S in particular is now also able to reproduce the qualitative progressions for all three slices.
However, even the already relatively good L25 benefits from the inclusion of sweeps as training points and is now practically on par with the L/D from the FF SM in most areas. The only exception is the lower range of vertical positioning between $-1 < (z/c)_{prop} < -0.625$, where there is a decrease in agreement; otherwise, however, the results are improved. For comparison, the SM purely trained with the sweep data fails totally in the prediction. The improvement of the L9S is therefore not a simple consequence of the sweep data, the orthogonality of the L9 sampling points is instead crucial for resolving the parameter space outside the sweeps.
The influence on excess efficiency is mixed. The L25 is improved for the detection of $(x/c)_{prop}$ and $(z/c)_{prop}$ and is now almost in line with the FF results. For θ, however, the sweep consideration leads to larger deviations at higher angles, but the position and size of the optimum are better approximated. The L9 does not benefit from the consideration of the sweeps, apart from the optimum position at $(z/c)_{prop}$. However, the changes relative to the optimum values remain relatively small.
Overall, it can be seen that with existing manual CFD sweeps, a comparatively small number of additional DoE sampling points are sufficient to represent the entire parameter space for DP positioning. In this case, 31 simulations were performed to calculate the sweeps, so the additional L9 sampling points correspond to an additional computational effort of approximately 1/3 and for the L25 extension of $\approx 80\%$. After analyzing the SM extended by the sweeps, it can be assumed that the results of 4 levels by an L16 orthogonal Taguchi array would fall between the results of the extended L9S and L25S and would probably be the best compromise between additional computing effort and quantitative and qualitative representation.

4 Conclusion and Outlook

The suitability of surrogate models for representing the large parameter space of propeller-wing interactions was analyzed in this study. Based on design of experiment sampling points, CFD simulations were performed using a 2.5D model. Orthogonal Taguchi arrays (L9 and L25) and a full factorial (FF) design were used. The CFD results became training points for creating SM. The SM output was validated with further CFD simulations alongside parameter sweeps outside the training points. The main findings are:

- For the resolution of the DP parameter space, SM with 5 levels lead to a close match with the CFD sweeps (L25 and FF). By using the Taguchi L25 array, 80% of the computational effort can be saved while maintaining practically the same quality in terms of aerodynamic efficiency and excess power. The influence of aerodynamic interactions via the streamwise and vertical propeller position and the inclination angle can be captured by using SM.
- The optimum positioning and inclination of the propellers can be identified by the SM in almost same precision as with CFD simulations. The predicted excess efficiencies deviate only very slightly by $\delta \approx 0.1\%$. The optimal propeller position is identified at approximately the same point in the parameter space.
- Three levels are insufficient for determining the DP parameter space. With an SM based on only three levels with an L9 array, the qualitative progression of the aerodynamic efficiency cannot be reproduced; however, the deviations in excess power are still small with $\delta \approx 0.2\%$.
- If manual sweeps are already available from an aerodynamic investigation, it is advisable to use them in combination with additional sampling points for the SM generation to cover the entire parameter space. In this way, even with an L9 array, the qualitative progression of the aerodynamic efficiency can be resolved. In contrast to using a FF design with 5 levels, this requires only 7.2% additional computing effort.
- If sweep data are not available, it is advantageous to spend the CFD simulations purely based on DoE sampling points. In this case, the original L25 shows better agreement than the sweep extended L9 with a lower number of simulations in total.

Overall, it was demonstrated that the parameter space for positioning DP propellers in front of a wing can be reproduced qualitatively and quantitatively by SM. The models trained with CFD data lead to comparatively similar results as CFD outside the training points. The use of CFD-trained SM in

aircraft design for the layout of DP aircraft is therefore valid. In the same manner it would be possible to include further parameter, however the number of simulations for an accurate representation by SM would also increase.
As a next step the use of a *Variable-Fidelity-Modeling Technique* will be tested to further improve the accuracy of the SM. This technique allows the combination of different CFD methods of different fidelity and computational time, whereby the accuracy of a surrogate model, primarily generated from low-fidelity results, can be enhanced by a few complex high-fidelity results. It is well known that while the ACD is able to resolve the qualitatively characteristics of the DP interaction, the lift increase is overestimated in comparison to time-accurate simulations. In the context of propeller simulation, a few time-accurate Actuator-Line (ACL) model results (L9) will thus be combined with a relatively larger number of ACD results (L25) in order to further improve the SM response for the aircraft design.

Remark

The CFD simulations were performed by M. Kern as part of the VELAN project, the surrogate model building and subsequent analysis by M. Schollenberger.

Acknowledgment

The authors gratefully acknowledge the Federal Ministry for Economic Affairs and Energy (BMWE) for funding this work in the framework of the research project VELAN (FKZ: 20E1919). The authors have no competing interests to declare that are relevant to the content of this article.

Supported by:

Federal Ministry for Economic Affairs and Energy

on the basis of a decision by the German Bundestag

References

[1] de Vries, R., Hoogreef, M., and Vos, R., Aeropropulsive efficiency requirements for turboelectric transport aircraft, In *AIAA Scitech 2020 Forum*, 2020, DOI: 10.2514/6.2020-0502.

[2] Drela, M. and Youngren, H., Xrotor download page, 2011, http://web.mit.edu/drela/Public/web/xrotor/.

[3] Firnhaber Beckers, M., Schollenberger, M., Lutz, T., Bongen, D., Radespiel, R., Florenciano, J., and Funes-Sebastian, D., Cfd investigation of high-lift propeller positions for a distributed propulsion system, 06 2022, DOI: 10.2514/6.2022-3217.

[4] Keller, D., Towards higher aerodynamic efficiency of propeller-driven aircraft with distributed propulsion, *CEAS Aeronautical Journal*, 12(4):777–791, 2021, DOI: 10.1007/s13272-021-00535-5.

[5] Raichle, A., Melber-Wilkending, S., and Himmisch, J., A new actuator disk model for the tau code and application to a sailplane with a folding engine, In Tropea, C., Jakirlic, S., Heinemann, H.-J., Henke, R., and Hönlinger, H., editors, *New Results in Numerical and Experimental Fluid Mechanics VI*, 2006, DOI: 10.1007/978-3-540-74460-3_7.

[6] Saves, P., Lafage, R., Bartoli, N., Diouane, Y., Bussemaker, J., Lefebvre, T., Hwang, J. T., Morlier, J., and Martins, J. R. R. A., SMT 2.0: A surrogate modeling toolbox with a focus on hierarchical and mixed variables gaussian processes, *Advances in Engineering Sofware*, 188:103571, 2024, DOI: https://doi.org/10.1016/j.advengsoft.2023.103571.

[7] Schollenberger, M., Kirsch, B., Lutz, T., Krämer, E., and Friedrichs, J., Aerodynamic interactions between distributed propellers and the wing of an electric commuter aircraft at cruise conditions, *CEAS Aeronautical Journal*, pages 1869–5590, 2024, DOI: 10.1007/s13272-023-00706-6.

[8] Schwamborn, D., Gerhold, T., and Heinrich, R., The dlr tau-code: Recent applications in research and industry, In *EC-COMAS CFD 2006 CONFERENCE*, 2006, https://elib.dlr.de/22421/.

[9] Stokkermans, T. C. A., Nootebos, S., and Veldhuis, L., Analysis and design of a small-scale wingtip-mounted pusher propeller, In *AIAA Aviation 2019 Forum*, 2019, DOI: 10.2514/6.2019-3693.

[10] Wolf, A., Bogdanski, S., Henes, D., and Lutz, T., Automatisierte prozesskette zur anwendung der taguchi-methode für die bestimmung von parametereinflüssen bei tau-rechnungen, Userguide, Universität Stuttgart, Institut für Aerodynamik und Gasdynamik, Stuttgart, Germany, Nov. 2011.